

1 **SUPPLEMENTARY MATERIAL**

2 **SNP discovery and Genotyping**

3 A detailed description of SNP discovery and genotyping is provided elsewhere  
4 (Stapley et al. 2008). In brief, the SNPs were identified using the QualitySNP  
5 software pipeline (Tang et al. 2006) from normalised cDNA sequences deposited in  
6 Genbank. We used the Illumina (San Diego) Golden Gate platform to genotype 354  
7 individuals at 876 SNPs (Stapley et al. 2008). SNP physical positions were obtained  
8 using BLAST (v2.7.1) (Altschul et al. 1997) to compare sequence containing the SNP  
9 (50-121 bp) against the zebra finch genome sequence  
10 ([http://genome.wustl.edu/pub/organism/Other\\_Vertebrates/Taeniopygia\\_guttata/assembly/Taeniopygia\\_guttata-3.2.4/](http://genome.wustl.edu/pub/organism/Other_Vertebrates/Taeniopygia_guttata/assembly/Taeniopygia_guttata-3.2.4/)). Stand-alone BLASTn was used with default  
11 parameter settings, except the expectation value (-e) was set to 1e-10 and the word  
12 size length (-W) was set to 25. In the few cases where SNP sequences had multiple  
13 hits, the best hit (lowest expectation value) was chosen provided the predicted  
14 location was consistent with the linkage map. SNPs that hit to unassembled contigs  
15 (denoted by “\_random” or ChrUn) were not included in the analysis.

17

18 ***Haplotype Inference***

19 There is general agreement that it is more accurate to employ a statistical procedure to  
20 infer haplotype phase when estimating LD from genotypic data (Weir 1979; Stephens  
21 et al. 2001; Slatkin 2008). There are two ways this can be done, with pedigree  
22 information or from population data (unrelated individuals). Although there are very  
23 good methods for estimating phase from population data, it is more accurate and  
24 efficient to use pedigrees (Stephens et al. 2001; Becker and Knapp 2002; Li and Jiang  
25 2005; Slatkin 2008). In addition, haplotypes inferred from population data are least

26 accurate when sample sizes are modest, as is the case in our study (Becker and Knapp  
27 2002). For this reason we chose to use a pedigree based estimate.

28

29 Phase can be inferred with pedigree information using statistical and rule based  
30 methods (e.g. Minimum Recombinant Haplotype Configuration, MRHC). Statistical  
31 methods perform very well and we chose to use SimWalk2, a Maximum Likelihood  
32 (ML) method. SimWalk is a well respected and well-used ML based statistical  
33 program and performs as well as more recently developed programs based on MRHC  
34 (Li and Jiang 2005). The main disadvantage of statistical procedures is that they are  
35 time consuming to run because of the large number of possible haplotype  
36 configurations that need to be considered. One way to reduce the time required is to  
37 split the pedigree into smaller sub families. Splitting the pedigree also helps to deal  
38 with marriage loops, which are present in our pedigree. Splitting the pedigree and  
39 duplicating individuals to create unrelated families is a common procedure employed  
40 in several programs (e.g. LINKAGE, FASTLINK, PedPhase). To split the pedigree  
41 into separate unrelated families we used CRIGEN implemented in CriMap.

42

43 CRIGEN includes some individuals in more than one family, artificially inflating the  
44 size of the pedigree to 468 individuals and 153 founders compared to the true  
45 pedigree of 354 individuals and 60 founders. To ensure that this inflation did not bias  
46 the results, estimates of LD obtained from the phased haplotypes with 153 founders  
47 were compared to those obtained from the unphased genotypes using the founders of  
48 the original pedigree (n=60). The correlation coefficient for pair wise  $r^2$  calculated  
49 from the two approaches was high ( $r = 0.95$ , Fig S1). LDmaps built using founder

50 diplotype data are also in close agreement with the LDmaps constructed from phased  
51 haplotypes (Fig S2).

52

### 53 **Modelling Linkage Disequilibrium**

54 Calculation, representation and interpretation of LD is a complex topic, which has  
55 been reviewed elsewhere (Devlin and Risch 1995; Pritchard and Przeworski 2001;  
56 Ardlie et al. 2002; Zhang et al. 2002; Zhao et al. 2007; Slatkin 2008). We have  
57 adopted an approach to modelling LD that will facilitate comparison with previous  
58 studies and make useful comparison between chromosomes within the zebra finch  
59 genome. To model the decline in LD, pair wise estimates of LD such as  $r^2$  and D' are  
60 commonly used. In this study we avoid the use of D' because this is sensitive to small  
61 sample sizes and  $r^2$  is generally considered the best statistic for SNP data (Pritchard  
62 and Przeworski 2001; Ardlie et al. 2002; Weiss and Clark 2002). The  $r^2$  statistic is the  
63 most useful in the context of mapping studies and it can be used to calculate the extent  
64 of useful LD to detect an association (Ardlie et al. 2002). The decline of  $r^2$  was  
65 modelled using Sved's equation as described in the body of the manuscript.

66

67 Despite the usefulness of the  $r^2$  statistic in the context of mapping, pair wise estimates  
68 of LD have some shortcomings. First, pair wise estimates between all markers are not  
69 independent, and as a result it is unclear how to combine these in a meaningful way  
70 and make inference (Pritchard and Przeworski 2001). Second, all pair wise metrics  
71 are, to varying degrees, confounded by either allele frequencies or the difference in  
72 allele frequencies between two markers (Hill and Robertson 1968) and/or differences  
73 in sample size (Slate and Pemberton 2007). This introduces potential problems when  
74 making comparisons between studies or between genomic regions. Therefore, in

75 addition to presenting analysis of  $r^2$ , LD was modelled using population genetics  
76 theory (Morton et al. 2001), and the Malécot equation (Malécot 1948).

77

78 **Estimation of Heterozygosity, GC content and Number of Genes**

79 Total LDU, number of genes, GC content and mean heterozygosity was calculated per  
80 megabase (Mb). The number of genes, their start stop positions and the GC content  
81 were obtained from Ensembl BioMart

82 (<http://www.ensembl.org/biomart/martview/fd0d38a6a0dcc351ca2e08912f50fbc8>)

83 using database Ensembl 56, dataset *Taeniopygia guttata* genes (taeGut3.2.4).

84 SNP heterozygosity ( $h_i$ ) was calculated for autosomal markers using

85 
$$h_i = Nh_i/N_i$$

86 where  $Nh_i$  is the number of founder individuals that were heterozygous at ith loci and

87  $N_i$  is the number of individuals typed at that loci.

88

89 **CpG Motifs**

90 Previous studies have identified that particular sequence motifs (CCTCCT,  
91 CTCTCCC, CCCCCC, CTCF Consensus - CCNCCNGGNGG) are correlated with  
92 recombination rate (Shifman et al. 2006; Groenen et al. 2009). The position of each  
93 motif was estimated using EMBOSS (Rice et al. 2000) and the number of motifs per  
94 megabase was calculated. These measures are highly correlated with GC content (Fig  
95 S3) so for simplicity we only used GC content in the analysis.

96 **References:**

97 Altschul S, Madden T, Schaffer A, Zhang JH, Zhang Z, Miller W, Lipman D. 1997.  
98 Gapped BLAST and PSI-BLAST: A new generation of protein database  
99 search programs. *Nucl. Acids Res.* **25**: 3389-3402.  
100 Ardlie KG, Kruglyak L, Seielstad M. 2002. Patterns of linkage disequilibrium in the  
101 human genome. *Nat. Rev. Genet.* **3**: 299-309.

102 Becker T, Knapp M. 2002. Efficiency of haplotype frequency estimation when  
103 nuclear family information is included. *Hum. Hered.* **54**: 45-53.

104 Devlin B, Risch N. 1995. A comparison of linkage disequilibrium measures for fine-  
105 scale mapping. *Genomics* **29**: 311-322.

106 Groenen MAM, Wahlberg P, Foglio M, Cheng HH, Megens H-J, Crooijmans RPMA,  
107 Besnier F, Lathrop M, Muir WM, Wong GK-S et al. 2009. A high-density  
108 SNP-based linkage map of the chicken genome reveals sequence features  
109 correlated with recombination rate. *Genome Res.* **19**: 510-519.

110 Hill WG, Robertson A. 1968. Linkage disequilibrium in finite populations.  
111 *Theoretical and Applied Genetics* **38**: 226-231.

112 Li J, Jiang T. 2005. Computing the Minimum Recombinant Haplotype Configuration  
113 from incomplete genotype data on a pedigree by integer linear programming. .  
114 *J. Comput. Biol.* **12**: 719-739.

115 Malécot G. 1948. Les Mathématiques de l'Hérédité. *Maison et Cie, Paris*.

116 Morton NE, Zhang W, Taillon-Miller P, Ennis S, Kwok PY, Collins A. 2001. The  
117 optimal measure of allelic association. *Proc. Natl. Acad. Sci. USA* **98**: 5217 -  
118 5221.

119 Pritchard JK, Przeworski M. 2001. Linkage disequilibrium in humans: Models and  
120 data. *Am. J. Hum. Genet.* **69**: 1-14.

121 Rice P, Longden I, Bleasby A. 2000. EMBOSS: The European Molecular Biology  
122 Open Software Suite. *Trends Genet.* **16**: 276-277.

123 Shifman S, Bell JT, Copley RR, Taylor MS, Williams RW, Mott R, Flint J. 2006. A  
124 high-resolution single nucleotide polymorphism genetic map of the mouse  
125 genome. *PLoS Biology* **4**: e395.

126 Slate J, Pemberton JM. 2007. Admixture and patterns of linkage disequilibrium in a  
127 free-living vertebrate population. *J. Evol. Biol.* **20**: 1415-1427.

128 Slatkin M. 2008. Linkage disequilibrium understanding the evolutionary past and  
129 mapping the medical future. *Nat. Rev. Genet.* **9**: 477-485.

130 Stapley J, Birkhead TR, Burke T, Slate J. 2008. A linkage map of the Zebra Finch  
131 *Taeniopygia guttata* provides new insights into avian genome evolution.  
132 *Genetics* **179**: 651-667.

133 Stephens M, Smith NJ, Donnelly P. 2001. A new statistical method for haplotype  
134 reconstruction from population data. *Am. J. Hum. Genet.* **68**: 978-989.

135 Tang JF, Vosman B, Voorrips RE, Van der Linden CG, Leunissen JAM. 2006.  
136 QualitySNP: a pipeline for detecting single nucleotide polymorphisms and  
137 insertions/deletions in EST data from diploid and polyploid species. *BMC  
138 Bioinformatics* **7**.

139 Weir BS. 1979. Inferences about Linkage Disequilibrium. *Biometrics* **35**: 235-254.

140 Weiss KM, Clark AG. 2002. Linkage disequilibrium and the mapping of complex  
141 human traits. *Trends Genet.* **18**: 19-24.

142 Zhang W, Collins A, Maniatis N, Tapper W, Morton NE. 2002. Properties of linkage  
143 disequilibrium (LD) maps. *Proc. Natl. Acad. Sci. USA* **99**: 17004-17007.

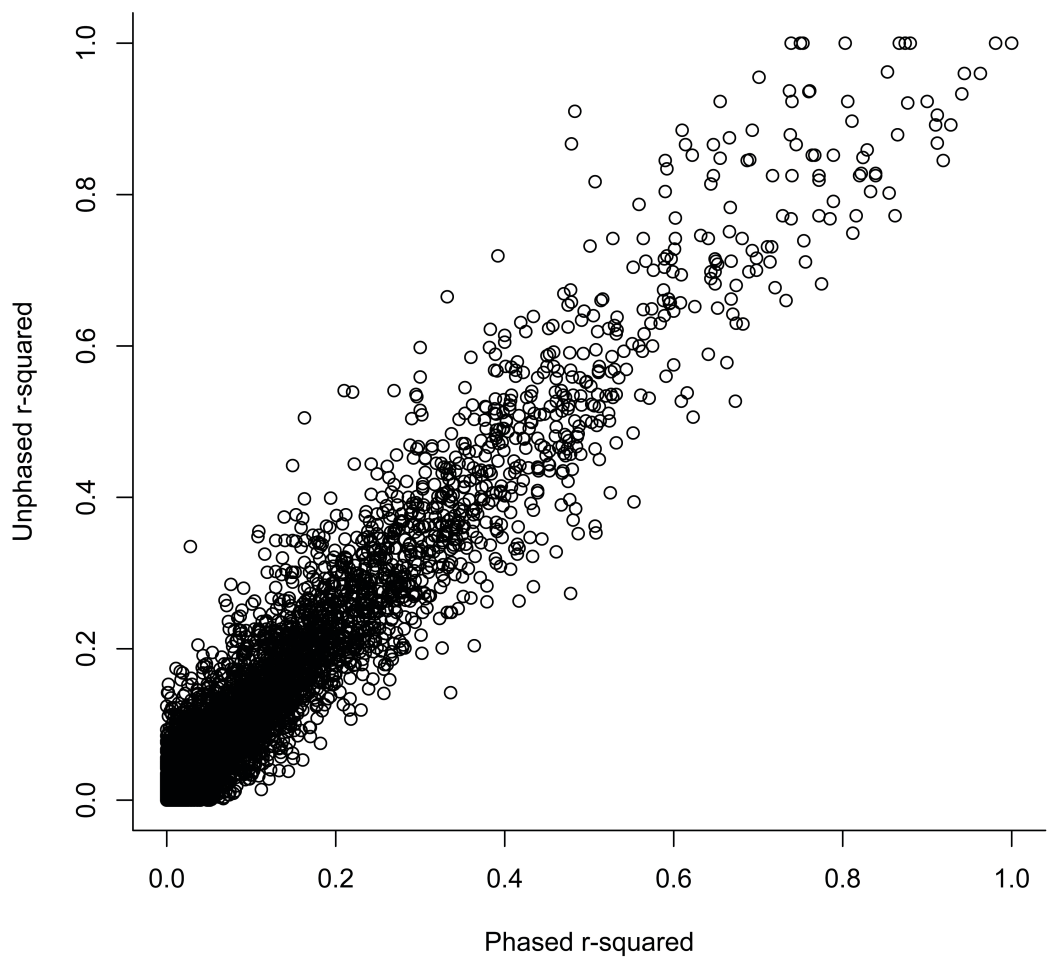
144 Zhao H, Nettleton D, Dekkers JCM. 2007. Evaluation of linkage disequilibrium  
145 measures between multi-allelic markers as predictors of linkage disequilibrium  
146 between single nucleotide polymorphisms. *Genet. Res.* **89**: 1-6.

147

148

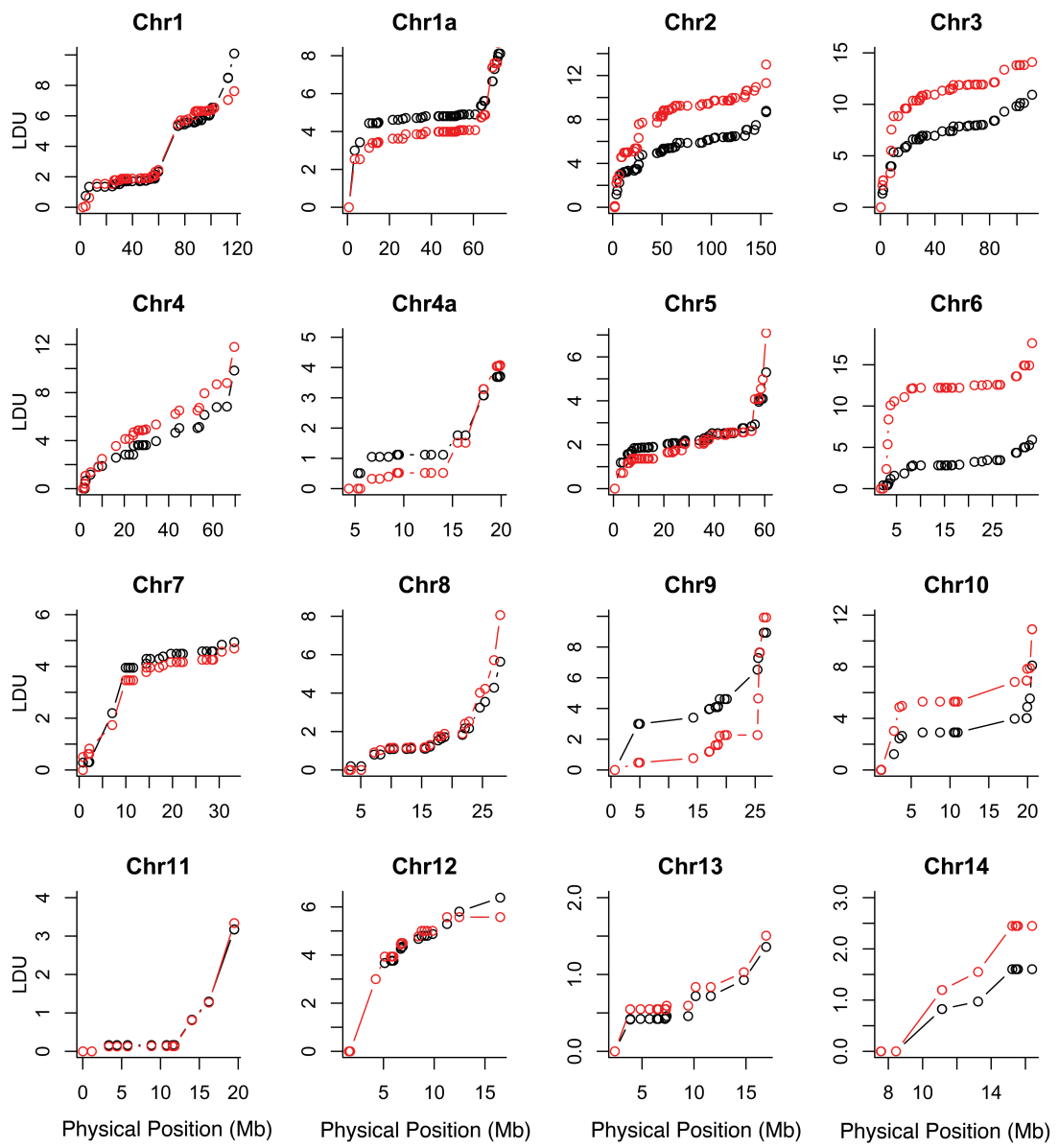
149

149 **Figure S1.** Pair wise LD ( $r^2$ ) estimated from phased haplotype data and unphased  
150 diplotype data (correlation coefficient = 0.95).  
151



152

153 **Figure S2.1.** LDmaps for chromosomes constructed using phased haplotypes (black  
154 and unphased genotypes (red).



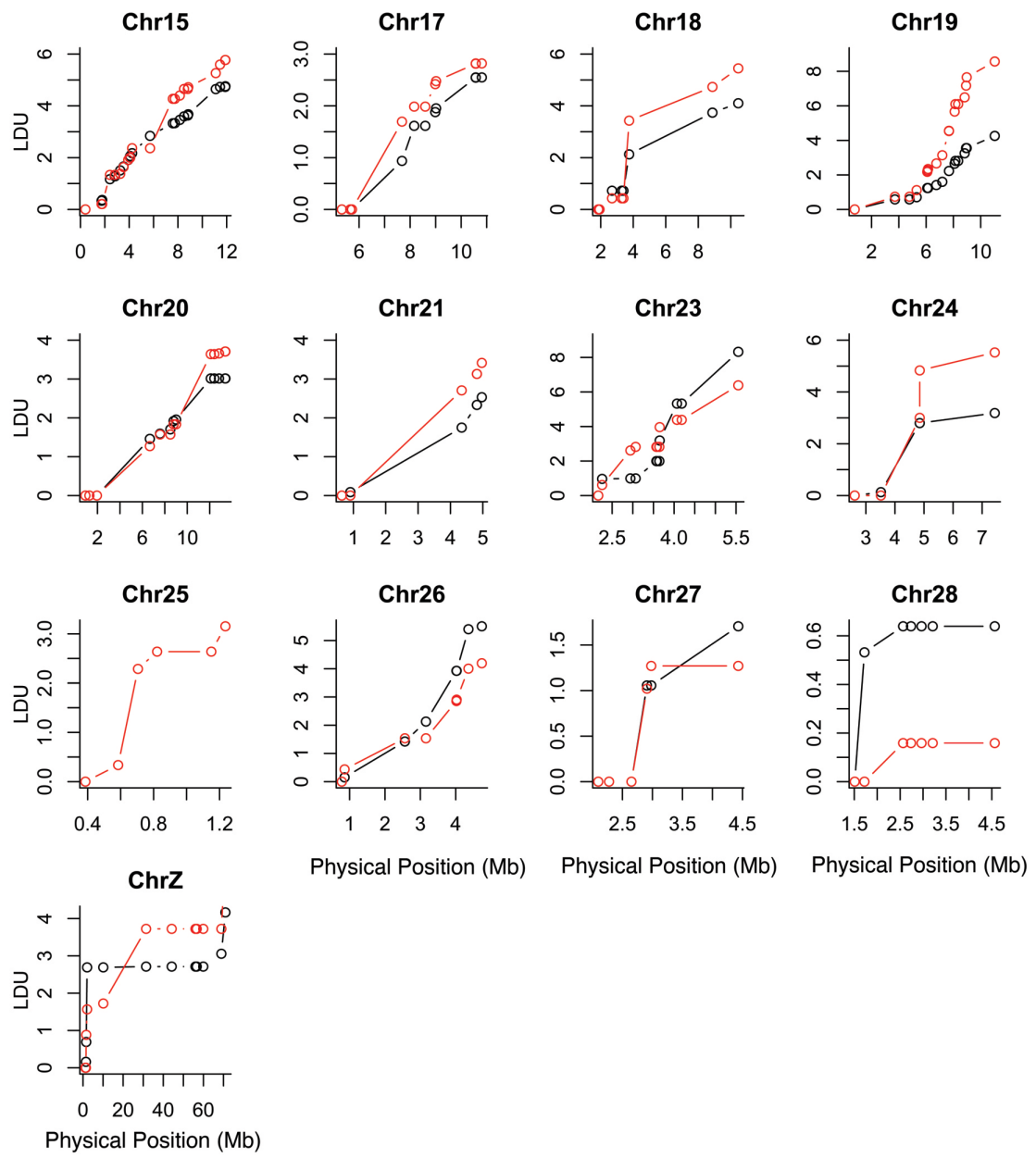
155

156

157

157 **Figure S2.2.** LDmaps for chromosomes constructed using phased haplotypes (black  
158 and unphased genotypes (red).

159



160

161

162

163

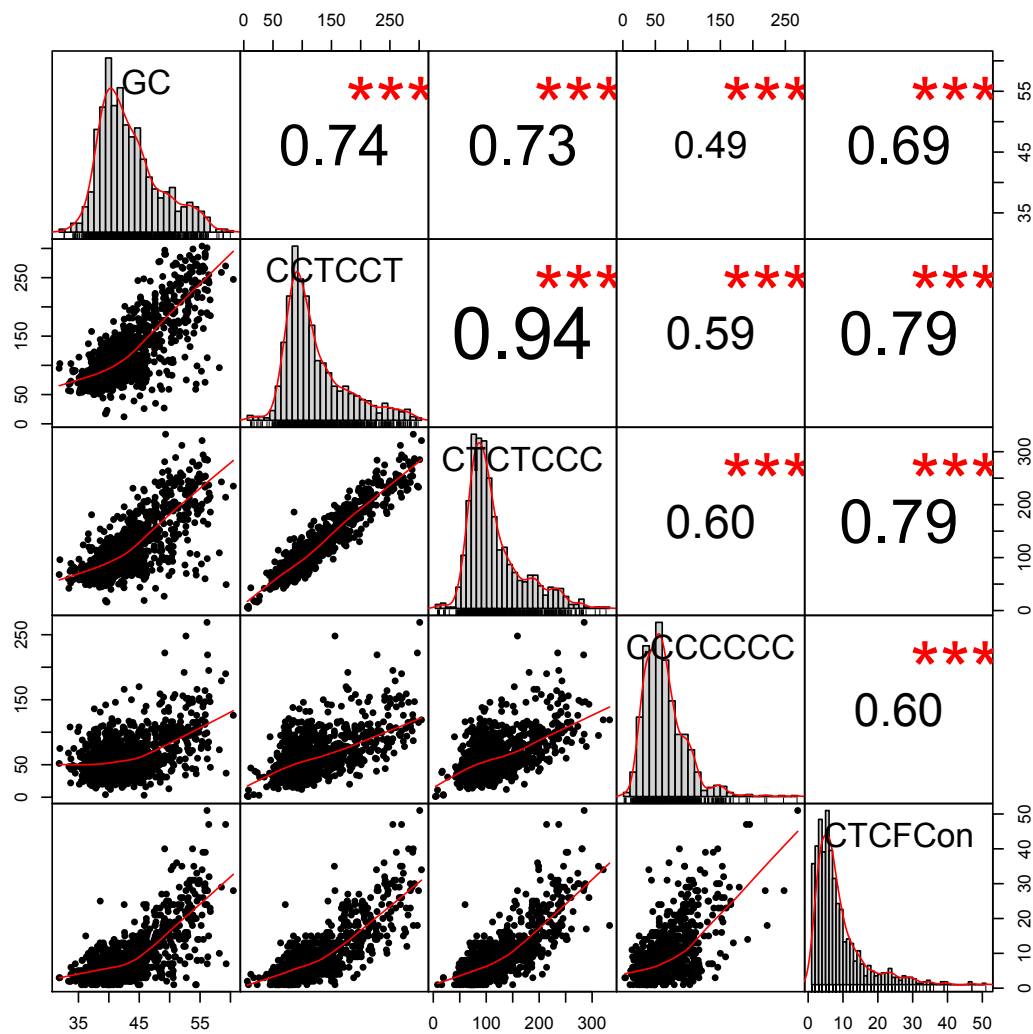
164

165

165

166 **Figure S3.** Correlation matrix of GC content and GC sequence motifs (CCTCCT, 167 CTCTCCC, CCCCCCCC, CTCF Con (CCNCCNGGNGG). Upper triangle of the 168 matrix gives correlation coefficient and significance level (0 \*\*\* <0.001 \*\* <0.05 \*), 169 on the diagonal is histograms of data and scatter plots on the lower triangle. All data 170 are log transformed.

171



172

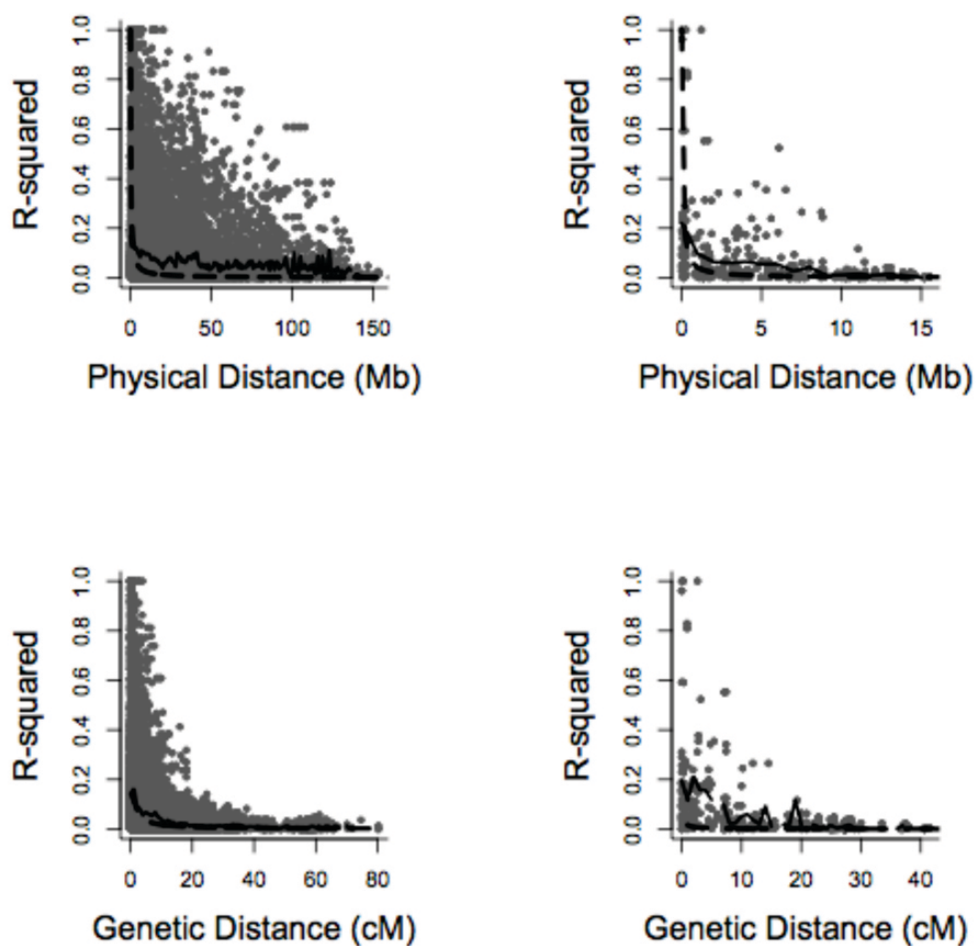
173

174

175

175 **Figure S4.** Linkage disequilibrium ( $r^2$ ) between syntenic pairs of SNPs plotted  
176 against: a) physical distance (Mb), solid line represents mean  $r^2$  for 1Mb bins, dashed  
177 line is the Sved's equation, for all the macrochromosome (left) and  
178 microchromosomes (right); b) genetic distance (cM), solid line represents mean  $r^2$  for  
179 1cM bins, dashed line is the Sved's equation, for all the macrochromosome (left) and  
180 microchromosomes (right).

181



182

183

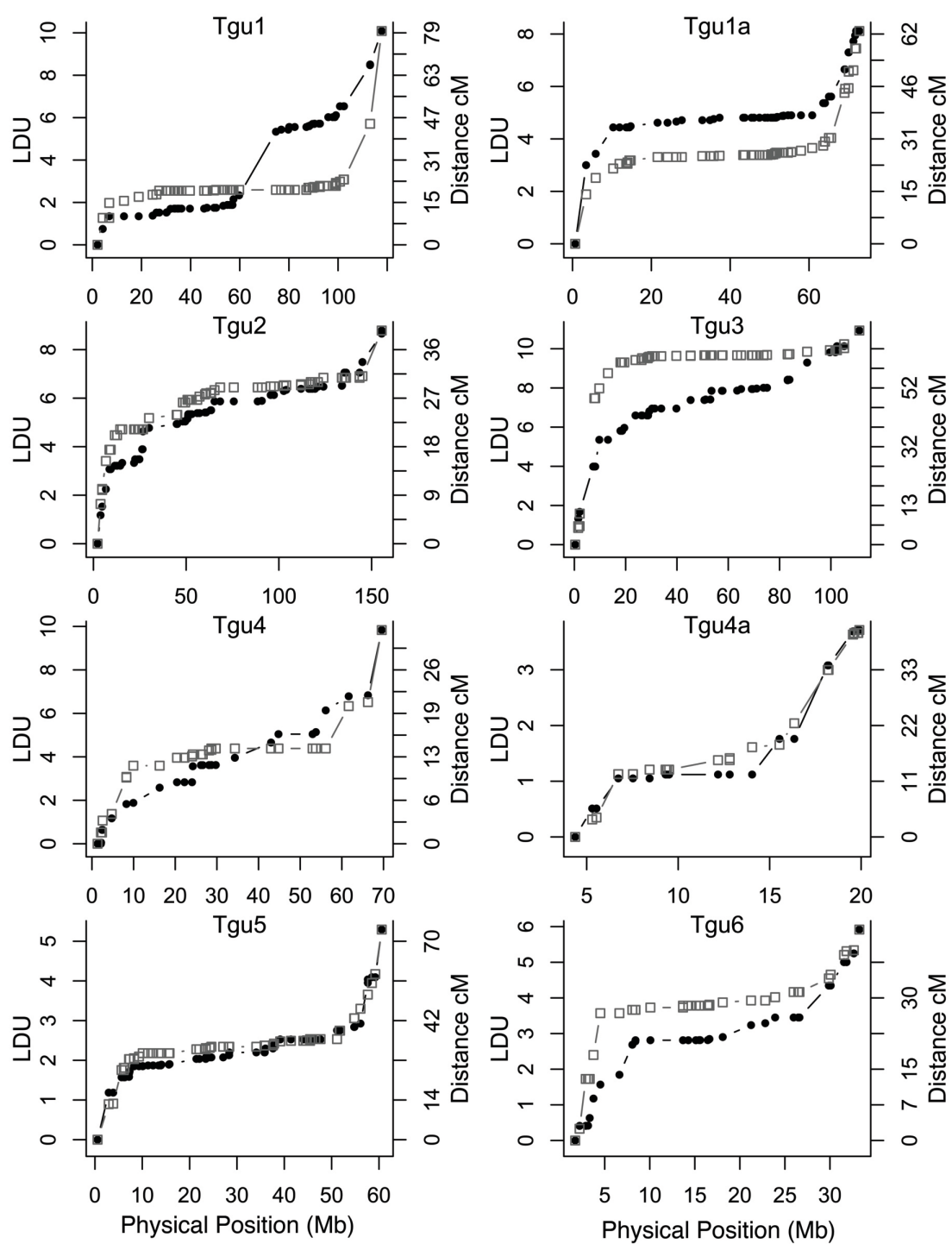
184

185

186

187

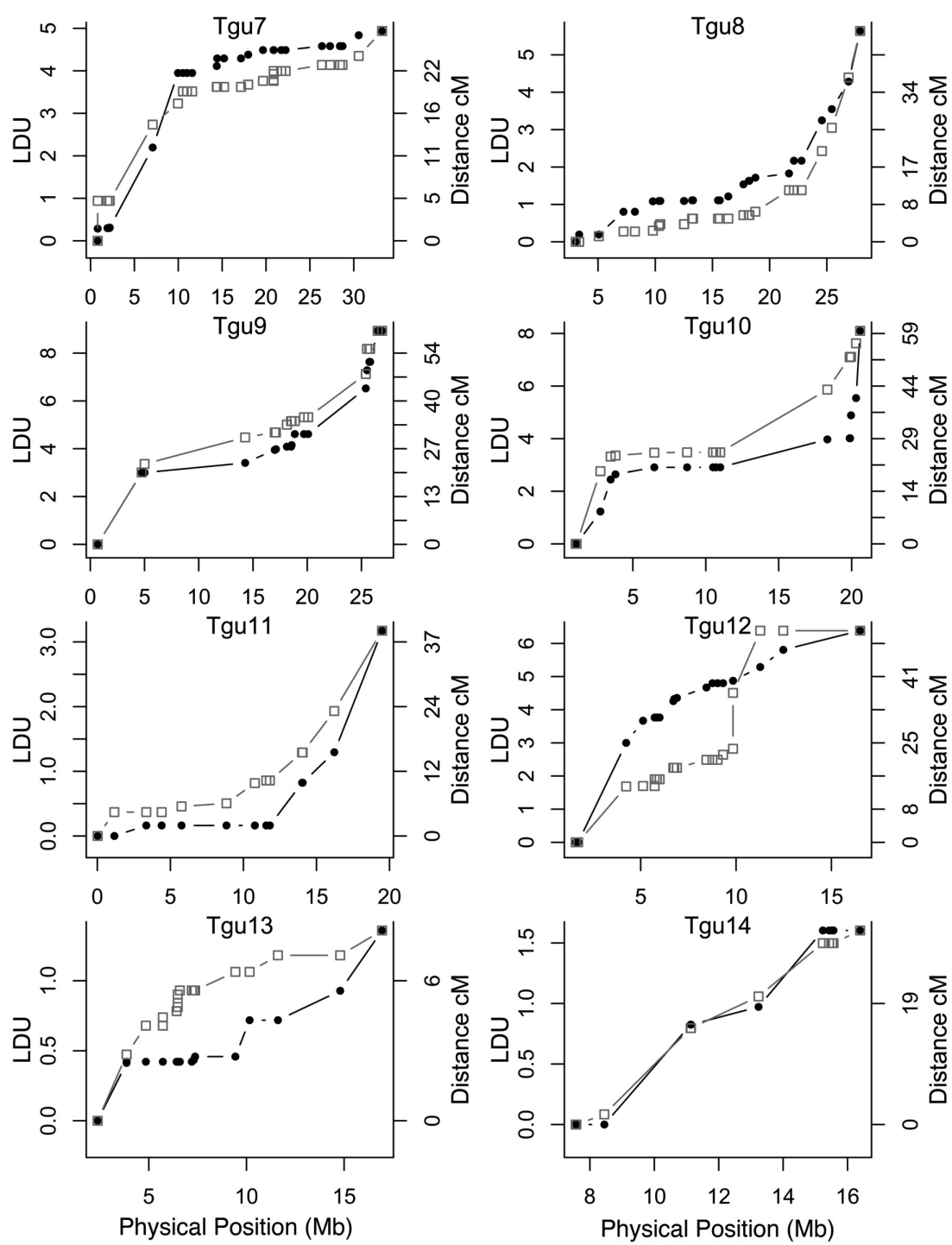
188  
189 **Figure S5.1.** LD maps (LDU) and genetic maps (cM) plotted against physical  
190 distance along each chromosome. Solid circles and black line indicate LD map and  
191 open red squares and red line indicate genetic map.



192  
193  
194

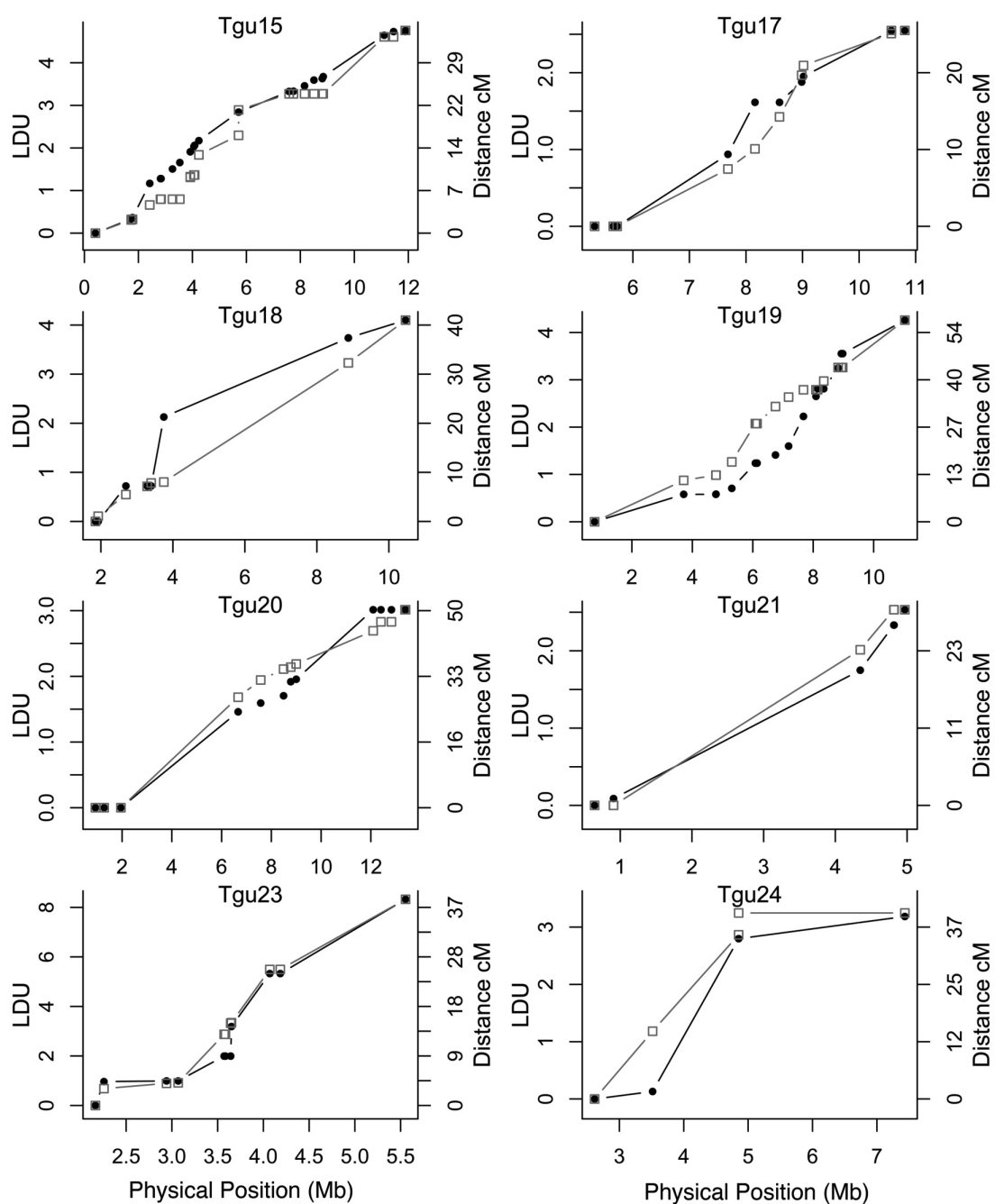
195

196 **Figure S5.2.** LD maps (LDU) and genetic maps (cM) plotted against physical  
197 distance along each chromosome. Solid circles and black line indicate LD map and  
198 open red squares and red line indicate genetic map.  
199



200  
201  
202  
203  
204  
205

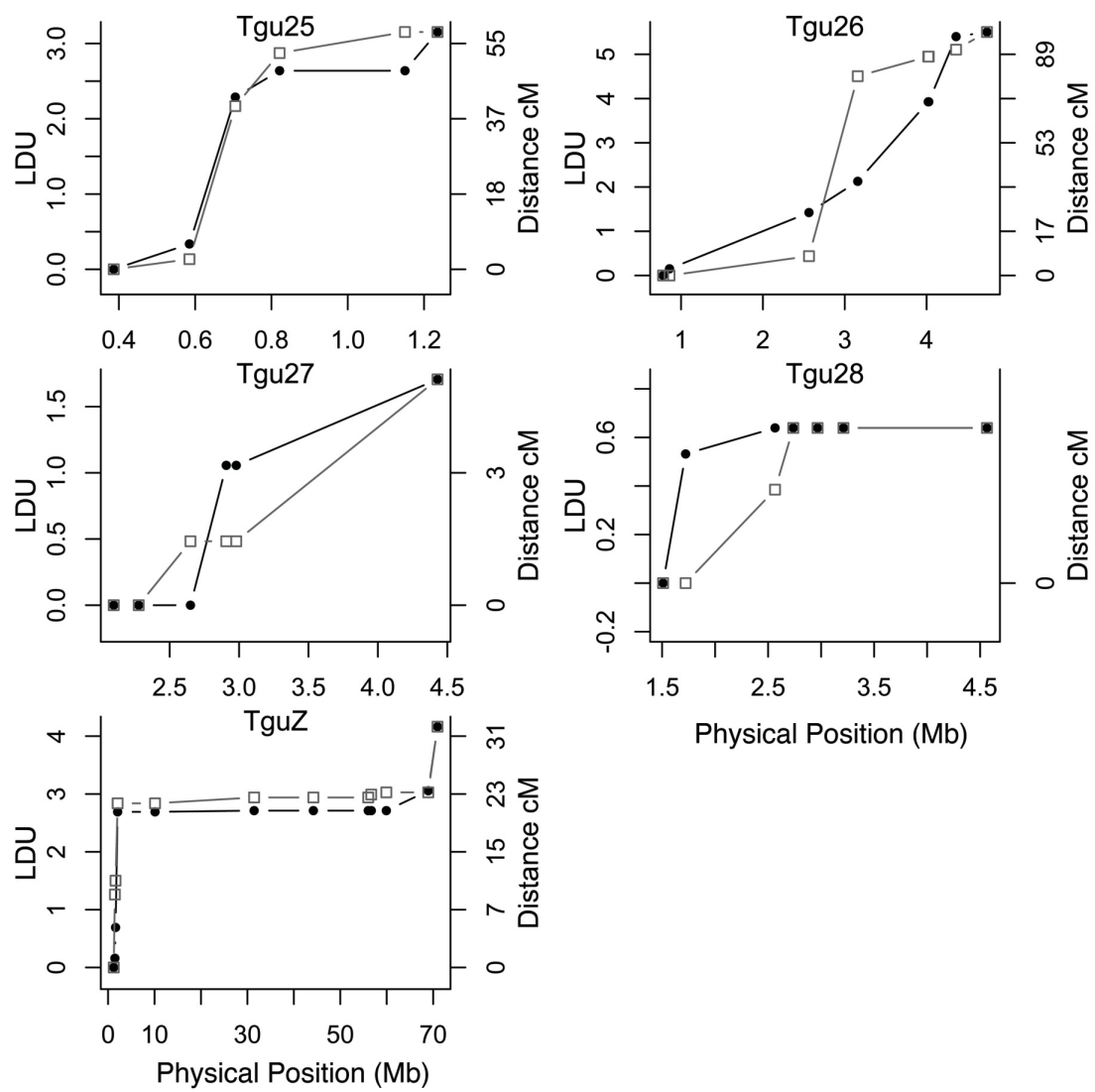
206 **Figure S5.3.** LD maps (LDU) and genetic maps (cM) plotted against physical  
207 distance along each chromosome. Solid circles and black line indicate LD map and  
208 open red squares and red line indicate genetic map.  
209



210  
211  
212  
213

214  
215  
216

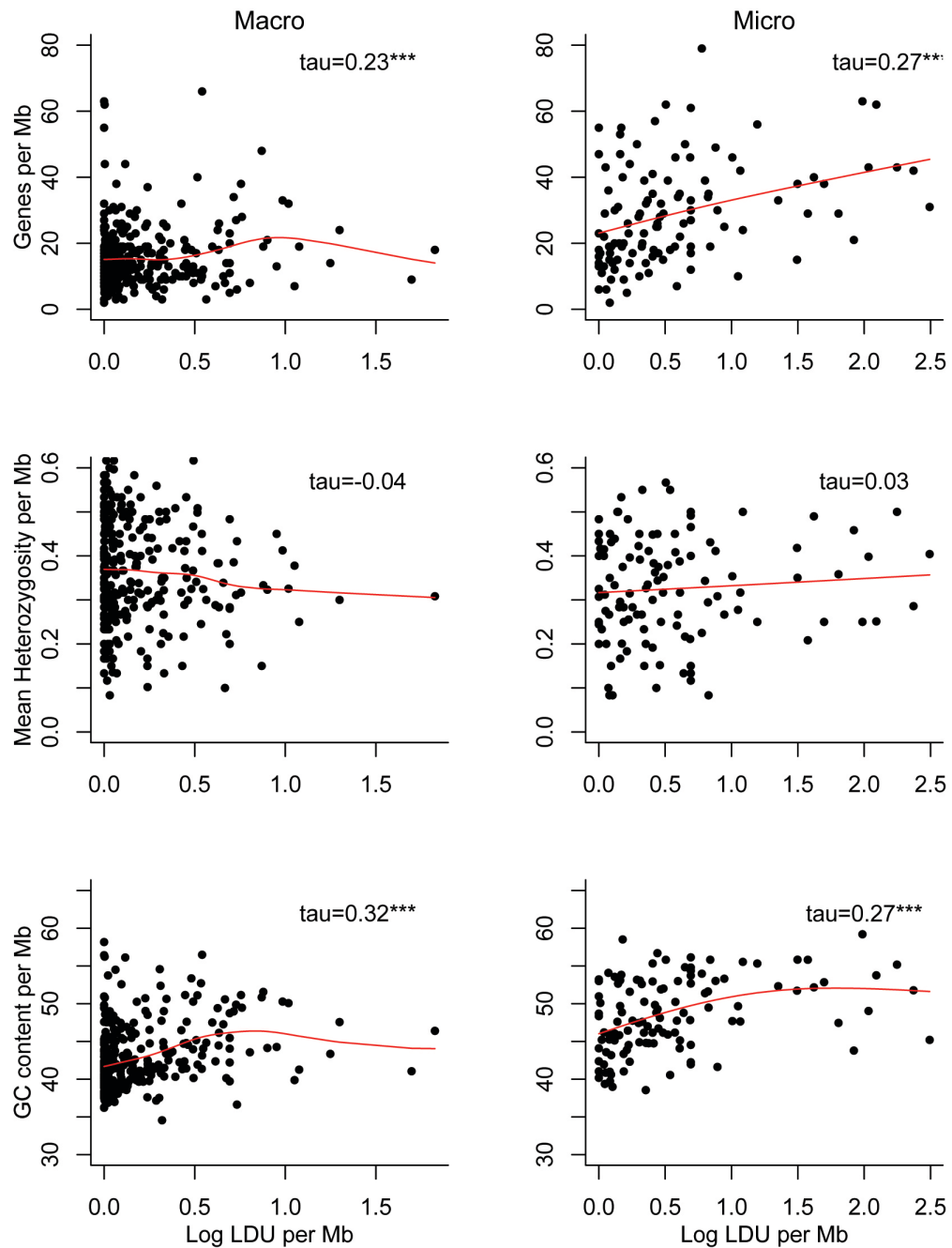
217 **Figure S5.4.** LD maps (LDU) and genetic maps (cM) plotted against physical  
218 distance along each chromosome. Solid circles and black line indicate LD map and  
219 open red squares and red line indicate genetic map.  
220



221  
222  
223  
224  
225  
226

227  
228  
229  
230

**Figure S6.** Relationship between sequence features per Megabase (Mb) (number of genes, GC content, heterozygosity) and log LDU per Mb. Correlation estimates based on Kendall's  $\tau$ , \*\*\* denotes  $p$ -value $<0.001$ ). Red lines are smoothed splines.



231  
232

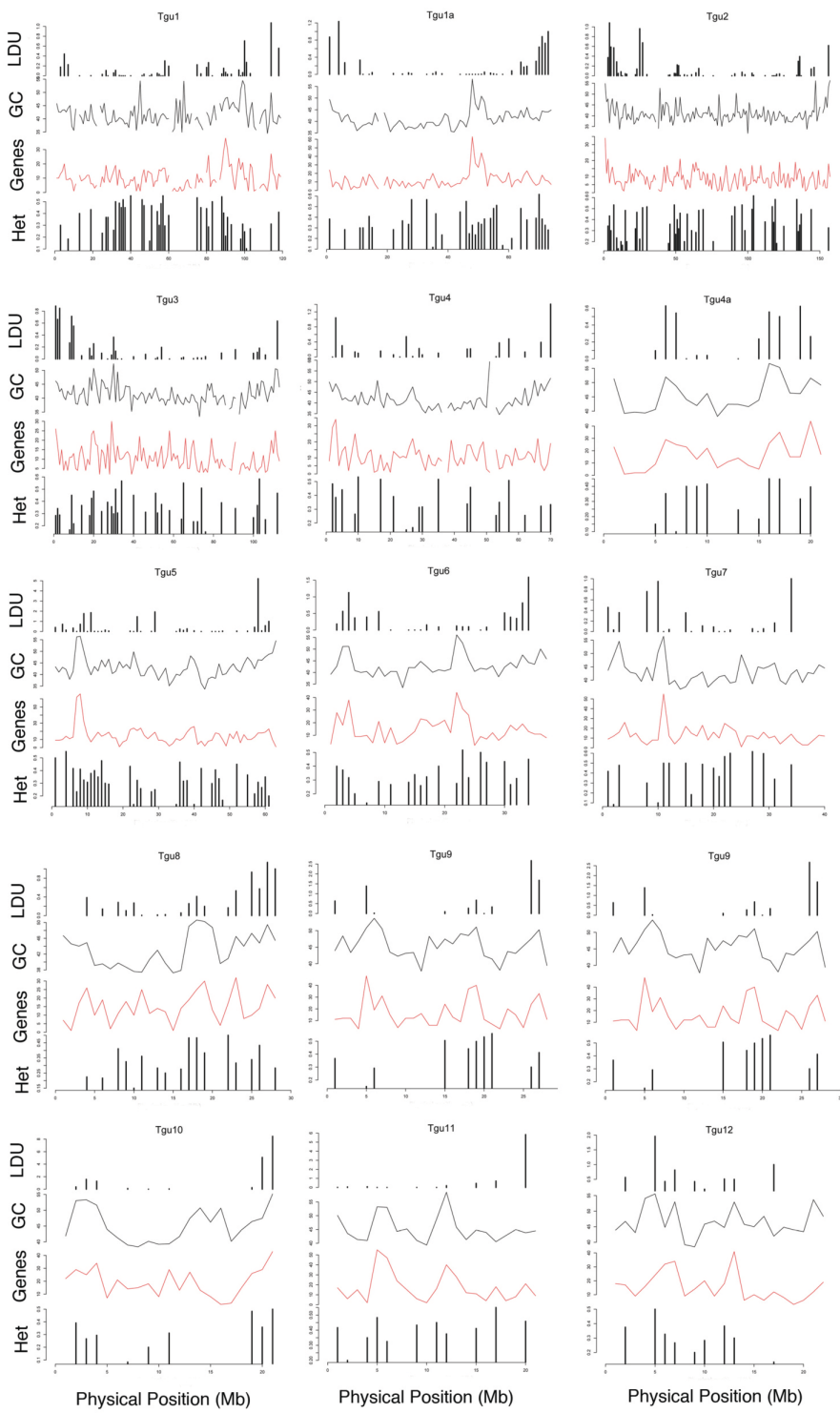
233

234

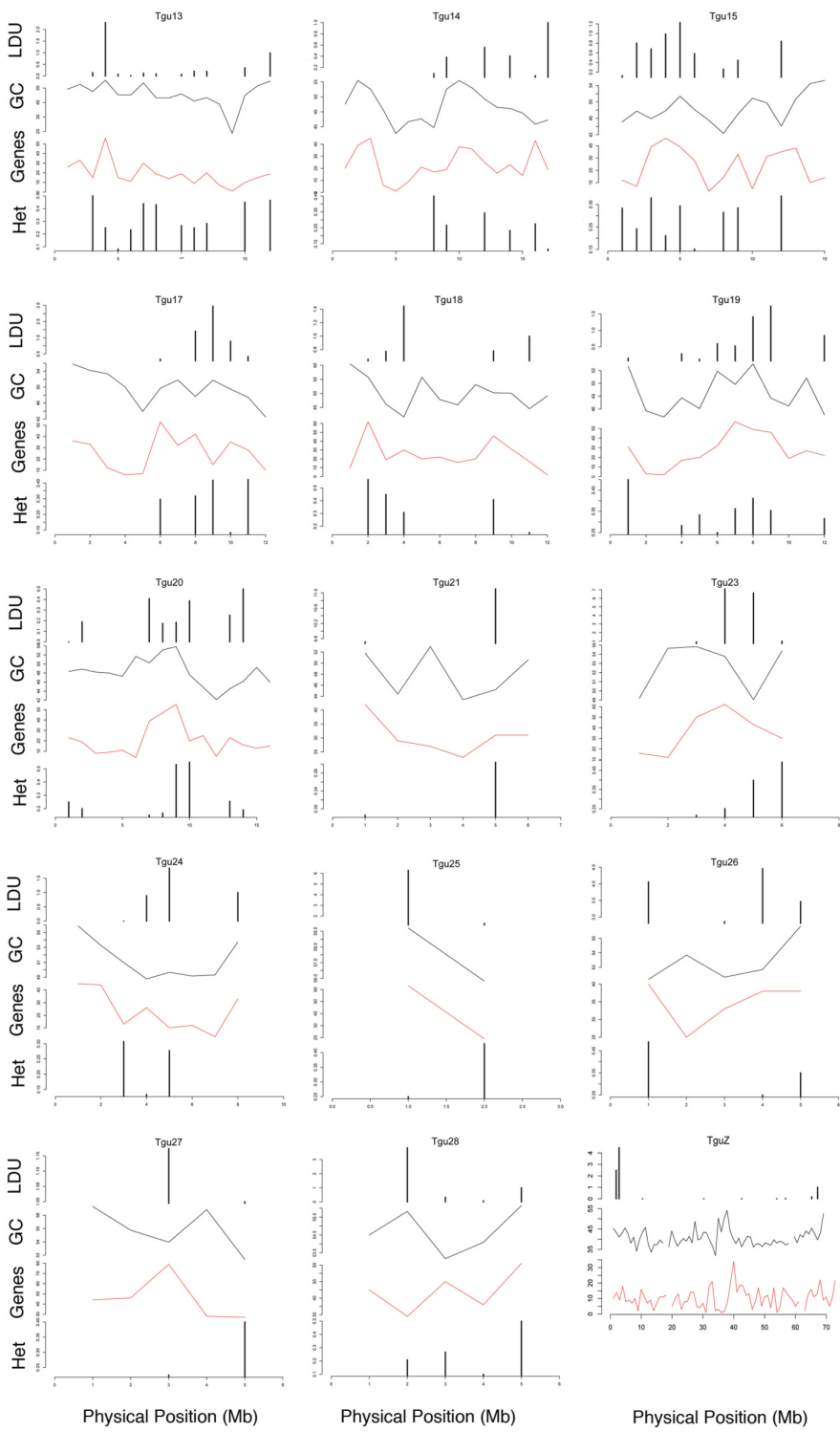
235

236

237 **Figure S7.1.** The total number of linkage disequilibrium units (LDU), GC content  
 238 (GC), number of genes (Genes) and mean heterozygosity (Het) per megabase (Mb)  
 239 along zebra finch chromosomes.



242      **Figure S7.2.** The total number of linkage disequilibrium units (LDU), GC content  
 243      (GC), number of genes (Genes) and mean heterozygosity (Het) per megabase (Mb)  
 244      along zebra finch chromosomes.  
 245



246

247